Figure S1

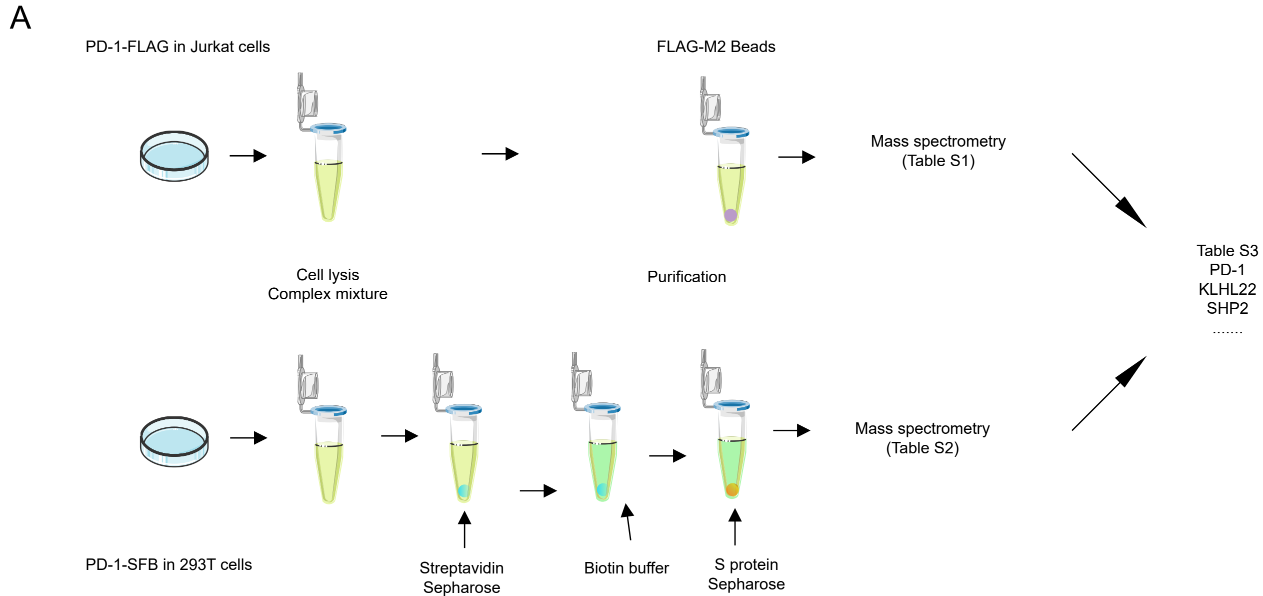

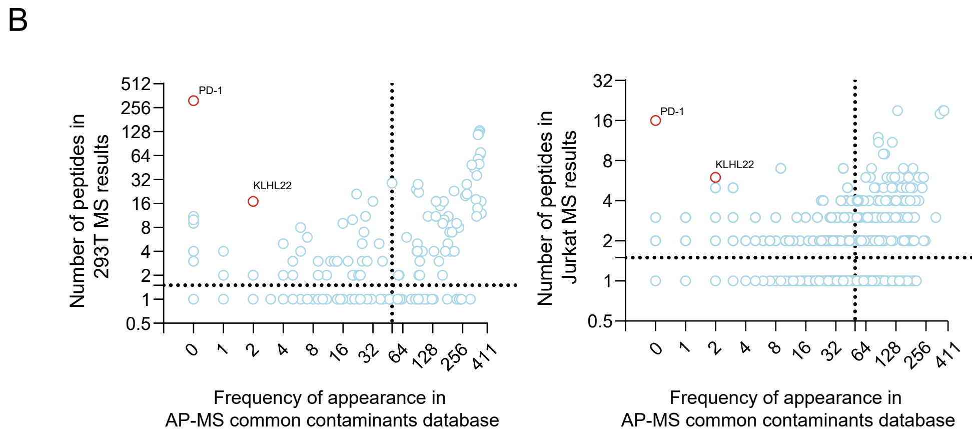

www.pnas.org/cgi/doi/10.1073/pnas.2004570117

Figure S1

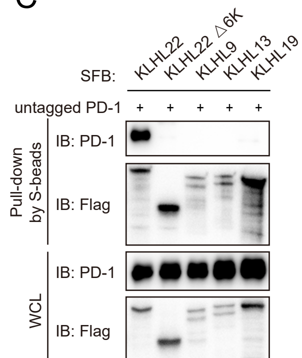

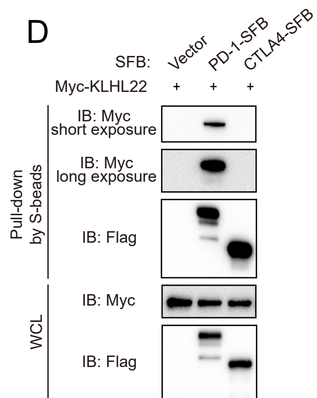

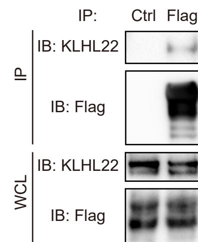

Figure S1. KLHL22 is a major PD-1-associated protein.

A. Workflow for protein purification and mass spectrometry. For stably expressing PD-1-Flag Jurkat cells, FLAG-M2 beads were used to purify PD-1 protein and its interactors. Mass spectrometry was performed to identify specific PD-1 interacting proteins. For stably expressing PD-1-SFB 293T cells, tandem affinity purification coupled with mass spectrometry was performed, which contains two steps of purification using streptavidin Sepharose and S-protein Sepharose, respectively.
B. Comprehensive analysis of MS results and AP-MS common contaminants databases Crapome. Frequency of proteins in MS results appearance in AP-MS common contaminants databases was showed. Protein appearance in 411 common contaminants databases was analyzed and frequency represents times of the protein appears in these databases. Number of peptides of corresponding protein was showed as well. The vertical dotted line indicates the frequency of 50. The further to the right a protein is, the more likely it is a junk protein. KLHL22 and PD-1 are significantly located in the upper left corner, suggesting that they are genuinely enriched and are hardly contaminants proteins.
C. Of the KLHL proteins, KLHL22 is the only one that interacts with PD-1. HEK293T cells were co-transfected with untagged PD-1 (PD-1 without an artificial tag) and PD-L1-SFB, SFB-KLHL22, SFB-KLHL9, SFB-KLHL13, or SFB-KLHL19. The cell lysates were subjected to pull-down assays with S-protein Sepharose and immunoblotted with the indicated antibodies.
D. The interaction of KLHL22 and PD-1 was confirmed in 293T cells, while CTLA4 showed no interaction with PD-1. PD-1-SFB or CTLA4-SFB was transfected respectively in 293T cells and purified using S-protein Sepharose.
E. The interaction of PD-1 and KLHL22 is confirmed in different salt ion concentrations. The interaction of PD-1-Flag and KLHL22 under 200 mM salt ion concentration. Protein G beads with IgG was used as a negative control. Jurkat cells were stimulated by PMA (50 ng/ml) and ionomycin (1 μM) for 12 hours.

Figure S2

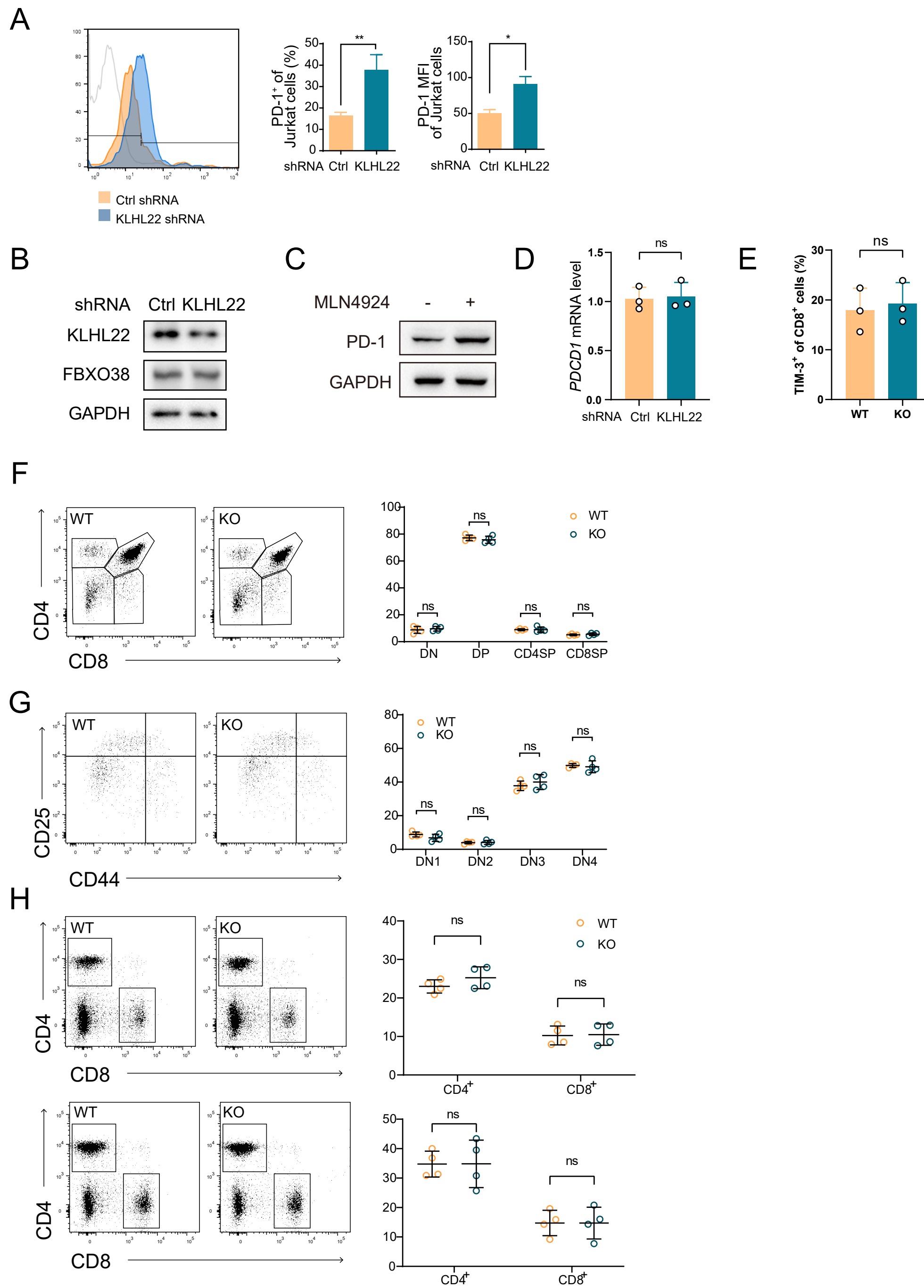

30 **Figure S2. Loss of KLHL22 leads to upregulation of PD-1 at the protein level.**

31 A. Depletion of KLHL22 increases PD-1 expression on the surface of Jurkat cells.
32 Lentivirus containing control or KLHL22-specific shRNA infected Jurkat cells that
33 stimulated with PMA (50 ng/ml) and ionomycin (1 μM) for 24h, followed by flow
34 cytometry to measure PD-1 expression on the cell surface.

35 B. Protein levels of KLHL22 and FBXO38 in control or KLHL22-shRNA virus infected
36 Jurkat cells.

37 C. Treatment of the Cullin family inhibitor MLN4924 leads to PD-1 accumulation. Jurkat
38 cells were treated with DMSO or MLN4924, and both groups were stimulated with
39 PMA (50 ng/ml) and ionomycin (1 μM) simultaneously. Immunoblotting was used to
40 detect PD-1 expression.

41 D. Transcription levels of *PDCD1* in Jurkat cells infected by lentivirus containing control
42 shRNA or KLHL22-specific shRNA showed no differences. Jurkat cells were
43 stimulated with anti-CD3 (1 μg/ml) and anti-CD28 (2 μg/ml). n=3 biological
44 independent repeats.

45 E. Cell-surface expression levels of TIM-3 in activated $CD8^+$ T cells from WT and
46 KLHL22 KO mice showed no differences. Naïve T cells from WT and KLHL22 KO
47 mice were stimulated with anti-CD3 (1 μg/ml) and anti-CD28 (2 μg/ml) antibodies for
48 24 hours. n=3 mice per group, ns, no significant, unpaired Student's t-test.

49 F. Percentages of $CD4^-CD8^-$ double-negative (DN), $CD4^+CD8^+$ double-positive (DP),
50 $CD4^+$ single-positive (CD4SP) and $CD8^+$ single-positive (CD8SP) cells out of the total
51 number of thymocytes from wild-type or KLHL22 KO mice.

52 G. Percentages of $CD44^+$ single-positive (DN1), $CD44^+CD25^+$ double-positive (DN2),
53 $CD25^+$ single-positive (DN3) and $CD44^-CD25^-$ double-negative (DN4) cells in $CD4^-$
54 $CD8^-$ cells from F.

55 H. Percentage of $CD4^+$ and $CD8^+$ T cells in lymph nodes (top) and spleen (bottom) of
56 wild-type and KLHL22 KO mice.

Figure S3

A

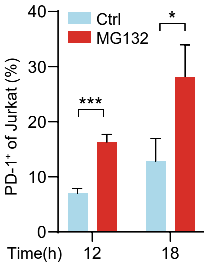

B

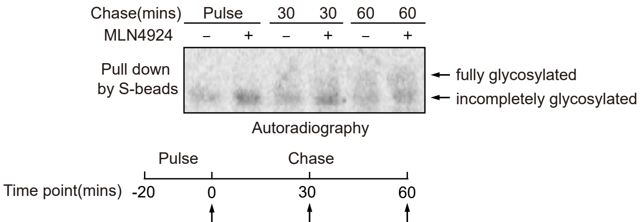

C

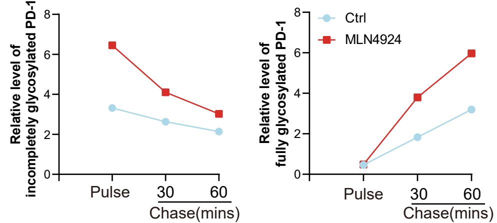

D

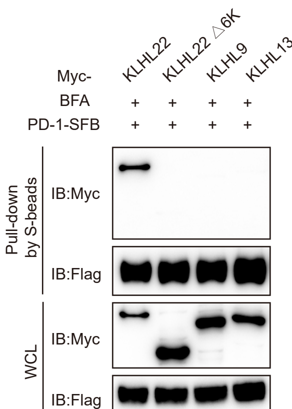

57 **Figure S3. KLHL22 mediates the degradation of PD-1 before it is transported to the cell**
58 **surface.**

59 A. Cell-surface levels of PD-1 in activated Jurkat cells with or without MG132 treatment
60 were detected by flow cytometry. Jurkat cells were stimulated with PMA (50 ng/ml)
61 /ionomycin (1 μM) and treated with MG132 (1 μM) for indicated hours. n=3 biological
62 independent samples, $^{**}P < 0.01$, unpaired Student's *t*-test.
63 B. MLN4924 increased PD-1 protein level in incompletely glycosylated state. 293T cells
64 were transiently transfected with PD-1-SFB and were pulse-labeled for 20 min with
65 [^{35}S] methionine and [^{35}S] cysteine and then chased with unlabeled methionine and
66 cysteine. MLN4924 was present during pulse and chase. Then cells were harvested at
67 the indicated times and PD-1-SFB was purified by S-beads pull-down and were
68 analyzed by autoradiography. Bands of different molecular weights represent different
69 glycosylation states of PD-1.
70 C. Quantification of the bands in S3C. With the chase time increased, the amount of
71 incompletely glycosylated PD-1 declined. Inversely, the amount of fully glycosylated
72 PD-1 increased gradually. MLN4924 (1 μM) treatment led to an increase of both
73 incompletely and fully glycosylated PD-1.
74 D. Incompletely glycosylated PD-1 specifically interacts with KLHL22, rather than
75 KLHL9 or KLHL13. 293T cells were transfected with PD-1-SFB and Myc-KLHL22,
76 Myc-KLHL22Δ6K, Myc-KLHL9, or Myc-KLHL13. All the groups were treated with
77 BFA (1 μM). The cell lysates were subjected to pull-down assays by S-protein
78 Sepharose and immunoblotted with the indicated antibodies.
79

Figure S4

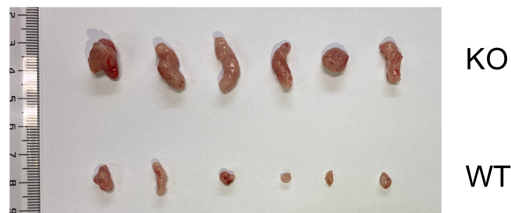

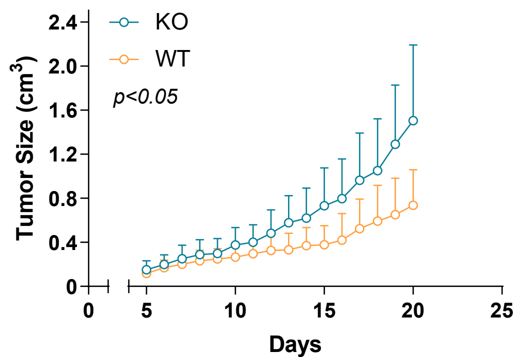

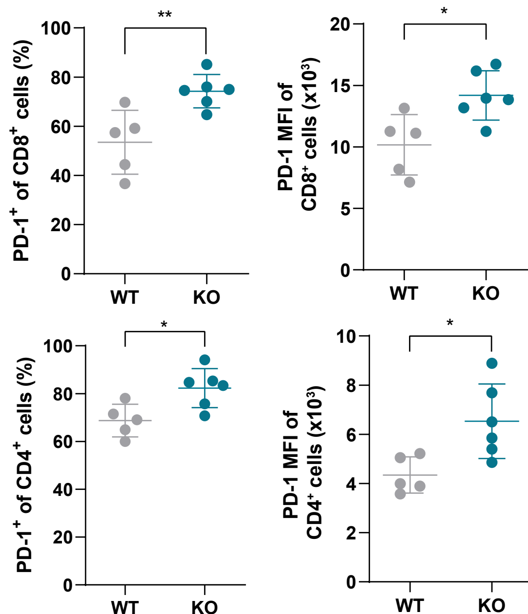

Figure S4. KLHL22 regulates T cell antitumor immunity.

A. KLHL22 KO mice showed faster tumor progression of MC38 tumor models. WT and KLHL22 KO mice were subcutaneously injected with MC38 cells. Tumors were isolated from mice sacrificed on day 17. n=6 mice per group.

B. KLHL22 KO mice showed faster tumor progression of MC38 tumor models. WT and KLHL22 KO mice were subcutaneously injected with MC38 cells and tumor growth was monitored over a period of 20 days. n=5 (WT) or 6 (KO) mice per group. $P < 0.05$, two-way analysis of variance (ANOVA). In order to analysis the phenotype of tumor-infiltrating T cells, tumor-bearing mice were euthanized on day 20.

C. PD-1 expression in tumor-infiltrating T cells from KLHL22 KO mice is significantly higher than that in cells from WT mice. Tumor-infiltrating T cells from WT and KLHL22 KO MC38 tumor-bearing mice were isolated on day 20 and subjected to flow cytometry. n=5 (WT) or 6 (KO) mice per group, * $P < 0.05$, ** $P < 0.01$, unpaired Student's *t*-test.

Figure S5

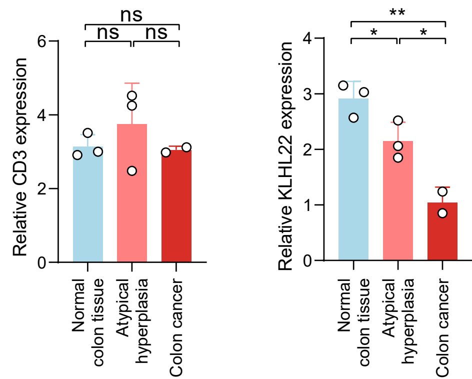

93 **Figure S5. T cell activation and the tumor microenvironment regulate KLHL22 expression.**
94 Quantification of the immunohistochemical staining intensity of CD3 and KLHL22 in the
95 cells indicated by the arrows. * $P < 0.05$, ** $P < 0.01$, unpaired Student's *t*-test.

Figure S6

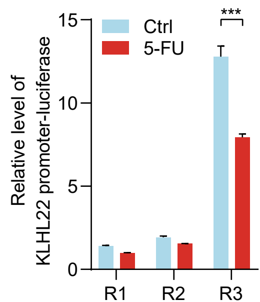

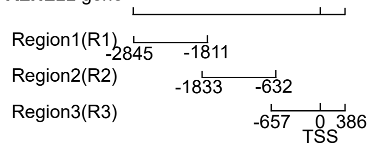

96 **Figure S6. 5-FU increases the expression of PD-1 by decreasing *KLHL22* mRNA levels.**

97 Region identification of KLHL22 promoter regulating KLHL22 expression under 5-FU
98 treatment. KLHL22 promoter-luciferase assay was performed under 5-FU treatment
99 (100 μM, 24 h). Three regions of KLHL22 presumed promoter were respectively cloned
100 into luciferase reporter plasmid and tested. *** $P < 0.001$, n=3, unpaired Student's *t*-test.

101

Supplementary Materials and Methods

Cells

HEK293T and B16F10 cells were cultured in DMEM supplemented with 10% fetal bovine serum and antibiotics (100 μg/ml streptomycin and 100 units/ml penicillin, MACGENE). Jurkat cells were cultured in RPMI 1640 supplemented with 10% fetal bovine serum and antibiotics. All cells were incubated at 37°C in a humidified ECSO incubator with 5% CO2.

Plasmids

cDNA of the PD-1, KLHL22, KLHL13, KLHL9, KLHL19, CTLA4, and PD-L1 open reading frames were subcloned into pDONR.201 (Invitrogen) as entry clones and subsequently transferred to gateway-compatible destination vectors for expression of untagged, N-tagged or C-tagged fusion proteins. All deletion and point mutants were generated by PCR and verified by sequencing.

KLHL22-targeted shRNA was inserted into the pLKO.1 vector with a GFP gene, which was used for sorting purposes. The shRNA sequences were as follows: 5′-GACTTCCTTTGTATCAGCTTA-3′ (#1) and 5′-GACTTCCTTTGTATCAGCTTA-3′ (#2). The packaging plasmids psPAX2 and pMD.2G for lentivirus production were purchased from Addgene. All constructs were confirmed by sequencing.

Immunoprecipitation and Western Blotting

Cells were lysed with NETN buffer (20 mM Tris-HCl [pH 8.0], 100 mM NaCl, 1 mM EDTA, and 0.5% Nonidet P-40) on a rotator at 4°C for 20 minutes. After cell debris was removed by centrifugation (14,000 rpm for 10 minutes at 4°C), the soluble fractions were collected and incubated with the indicated beads for 4 hours at 4°C. Then, the beads were washed three times with NETN buffer and boiled with 2× SDS loading buffer at 100°C for 8 minutes. The samples were then subjected to SDS-PAGE and immunoblotting with specific antibodies. The beads used were as follows: S protein agarose (Merck Millipore), FLAG-M2 beads (Sigma), and Protein A beads (GE life).

Lymphocyte, Splenocyte and Thymocyte Preparation

A total of six axillar, brachial and inguinal lymph nodes were dissected from each mouse. Single-cell suspensions from the thymus, spleen and the pooled six lymph nodes were prepared by grinding the organs with a 1-ml syringe plunger against a 70-µm cell strainer into 5 ml of RPMI 1640 (Gibco). Red blood cells were lysed with Ack lysis buffer (150 mM NH4Cl, 10 mM KHCO3 and 0.1 mM EDTA) for 5 minutes at room temperature followed by quenching with RPMI 1640, after which the sample was centrifuged and resuspended in 5 ml RPMI 1640.

RT-qPCR

Total RNA was extracted with TRIzol (Life Technologies) from the indicated cells and subjected to RT-qPCR using gene-specific primers. The primer sequences used were shown in Table S1

KLHL22 siRNA

Specific siRNA targeting human KLHL22 (KLHL22 siRNA) was designed according to the human KLHL22 cDNA sequence by Su Zhou Ji Ma (China). The sequences were shown in Table S1.

Flow Cytometry

Flow cytometry analysis was performed on a FACSCanto flow cytometer (BD Biosciences) with FACSDiva software (BD Biosciences). FlowJo VX was used for analysis. Cell surface expression levels of PD-1 were measured by flow cytometry with anti-PD-1 antibody. Intracellular levels of KLHL22 were measured by fixing and permeabilizing the cells before treatment with a fluorescently labeled KLHL22 antibody.

Isolation and Effector Function Analysis of Mouse Peripheral T Cells

Peripheral naïve $CD3^+$ cells were isolated from the mouse spleen by negative selection magnetic beads (Miltenyi Biotec). $CD3^+$ cells were stimulated with plate-bound anti-

CD3 and soluble anti-CD28 as indicated. To measure cytokine secretion, 5 μg/ml BFA was added 4 hours before cells were collected to block cytokine transport.

Pulse-chase Metabolic Labeling.

24 hours after PD-1 transfection, HEK-293T cells were incubated for 30 min in cysteine- and methionine-free DMEM containing 10% dialyzed FCS. Tran ^{35}S-label (40 μCi) was then added to the medium for the pulse period indicated in the figure legends, and cells were washed by PBS and were chased for various times with DMEM containing 10% full FCS and unlabeled methionine and cysteine. MLN4924 was present during pulse and chase. Then cells were harvested at the indicated time and PD-1-SFB was purified by S protein agarose and was analyzed by autoradiography.

Immunohistochemistry Staining

Tissues from humans and mice were formalin-fixed, paraffin-embedded and sectioned (5 μm thickness). The sections were deparaffinized with xylene and rehydrated with ethanol. Then, 3% hydrogen peroxide was added for 30 minutes at room temperature to eliminate endogenous peroxidase, after which the sections were subjected to antigen retrieval in sodium citrate (pH 6.0) for 20 minutes in a 100°C water bath. The specimens were then incubated with primary antibodies at 4°C overnight. The PV9000 2-step plus poly-HRP anti-mouse/rabbit IgG and PV6001 2-step plus poly-HRP anti-rabbit/goat IgG detection systems (Zhong Shan Jin Qiao) were applied. Diaminobenzidine (DAB) was used as a substrate (ChemMate Detection Kit, DAKO, Glostrup, Denmark), and hematoxylin was used as a counterstain.

Proximity Ligation Assay (PLA)

The KLHL22-PD-1 interaction was examined with reagents from Duolink PLA (Sigma). Cells were seeded onto cover slips and then fixed, blocked and stained with primary antibody and secondary antibody harboring short nucleotide sequences. Oligonucleotides were ligated at 37°C, and rolling circle replication with fluorescent nucleotides was performed for 100 minutes. The interaction was visualized with a confocal microscope.

Statement of Informed Consent Procedures

We submitted and approved the review application of this experiment to the Ethical Review Committee of Peking University People's Hospital. Then we informed the patient about the research background, purpose, steps, risks and benefits, and gave him/her enough time to read the informed consent form, discuss with others, and we answered his/her questions about the research. We have informed the subject when they encounter research-related problems, they can contact the doctor at any time. When encountering problems related to their own rights and interests, the subject can contact the Ethical Review Committee of Peking University People's Hospital at any time; we have informed the subject that he/she can withdraw from this study without any reason. The entire experiment was carried out under ethical principles such as the Declaration of Helsinki and International Ethical Guidelines for Biomedical Research Involving Human Subjects.

Table S1 Materials Table

Materials used in this study.

Reagent or Rresource	Source	Identifier
Antibodies		
Rabbit anti-PD-1	Boster	Cat#:PB0165
Mouse anti-PD-1	eBioscience	Clone:J116; Cat#: 14-9989-82
Mouse anti-Flag	Sigma-Aldrich	Clone:M2; Cat#:F3165
Rabbit anti-KLHL22	PROTEINTECH	Cat#: 16214-1-AP
Mouse anti-GAPDH	SUNGENE BIOTECH	Clone:1C4; Cat#:KM9002T
Mouse anti-c-Myc	SUNGENE BIOTECH	Clone:22E8; Cat#:KM8003
Mouse anti-ubiquitin	SANTA CRUZ	Clone:P4D1; Cat#:sc-8017
Mouse anti-PD-1	Sigma-Aldrich	Clone:7A11B1; Cat#:SAB3500122
Mouse anti-PD-1	BioXCell	Clone:RMP1-14; Cat#:BE0146
Rabbit anti-CD28	Abcam	Clone:EPR22076; Cat#:ab243228
Rabbit anti-CTLA4	Bioss Antibodies	Cat#:bs-10006R
Rabbit anti-CD3e	Sino Biological	Cat#: 108567-T08
Anti-mouse CD279 (PD-1) -APC/Cy7	BioLegend	Clone:29F.1A12; Cat#:135223
Anti-mouse CD279 (PD-1) -FITC	BioLegend	Clone:29F.1A12; Cat#:135213
Anti-human CD279 (PD-1) -APC	eBioscience	Clone:MIH4; Cat#: 17-9969-41
Anti-mouse CD3-APC	eBioscience	Clone: 17A2; Cat#:17-0032-80
Anti-mouse CD3e-PE	Invitrogen	Clone: 145-2C11; Cat#:12-0031-85
Anti-human CD3-PE-Cyanine7	eBioscience	Clone:OKT3; Cat#:25-0037-41
Anti-mouse CD4-PE	eBioscience	Clone:GK1.5; Cat#:12-0041-81
Anti-mouse CD4-APC	eBioscience	Clone:GK1.5; Cat#:12-0041-81
Anti-human CD4-PE	BD Pharmingen	Clone:L200; Cat#:550630
Anti-mouse CD8a-PE	Invitrogen	Clone:53-6.7; Cat#:MA1-10304
Anti-mouse CD8a-APC	eBioscience	Clone:53-6.7; Cat#:MA1-10302
Anti-mouse CD8a-APC-Cyanine7	eBioscience	Clone:53-6.7; Cat#:A15386
Anti-human CD8-APC	eBioscience	Clone:RPA-T8; Cat#:561953

Anti-mouse CD44-FITC	eBioscience	Clone:IM7; Cat#:11-0441-81
Anti-mouse CD25-PerCP-Cy™5.5	BD Pharmingen	Clone:PC61; Cat#:551071
Anti-mouse CD45-PE-Cyanine7	eBioscience	Clone:30-F11; Cat#:25-0451-82
Anti-mouse CD223 (LAG-3) -PE-Cyanine7	eBioscience	Clone:3DS223H; Cat#:25-2239-42
Anti-mouse IFNγ-APC-Cy™7	BD Pharmingen	Clone:XMG1.2; Cat#:561479
Anti-mouse TNFα-APC	BD Pharmingen	Clone:MP6-XT22; Cat#:561062
Anti-mouse Granzyme B-FITC	Invitrogen	Clone:NGZB; Cat#:11-8898-80
Anti-human KLHL22-PE	Bioss Antibodies	Cat#:bs-7807R-PE
Anti-mouse TIM-3-BV421	BD Horizon	Clone:CD366; Cat#:565562
Mouse anti-Rabbit IgG (Light Chain), HRP	Easybio	Cat#: BE0107
Bacterial and Virus Strains		
shRNA lentivirus	Genechem	
Biological Samples		
Human colorectal carcinoma tissues and blood samples	Peking University People's Hospital, Beijing, China	
Tissue microarrays	Peking University People's Hospital, Beijing, China	
Chemicals		
MG132	Sigma-Aldrich	Cat#:474787
MLN4924	Selleck	Cat#:S710903
Brefeldin A (BFA)	Selleck	Cat#:S704604
Cycloheximide (CHX)	HARVEYBIO	Cat#:C21865
5-Fluorouracil (5-FU)	HARVEYBIO	Cat#:F21691
PMA	Sigma-Aldrich	Cat#:P1585
Ionomycin	Sigma-Aldrich	Cat#:407952
Etoposide	HARVEYBIO	Cat#:HZB0098
Olaparib	Selleck	Cat#:S1060
Hydroxyurea (HU)	HARVEYBIO	Cat#:HZB0269
Irinotecan HCl Trihydrate (CPT-11)	Melonepharma	Cat#:MB1126
Mitomycin C (MMC)	Coolaber	Cat#:COL-CM7391
Critical Commercial Assays		
Duolink™ In Situ PLA® Probe Anti-Rabbit PLUS	Sigma-Aldrich	Cat#:DUO92002
Duolink™ In Situ PLA® Probe Anti-Mouse MINUS	Sigma-Aldrich	Cat#:DUO92004
Duolink™ In Situ Detection Reagents Red	Sigma-Aldrich	Cat#:DUO92008
Minute™ Golgi Apparatus Enrichment Kit	Invent biotech	Cat#:GO-037
CD3e MicroBead Kit	Miltenyi Biotec	Cat#:130-094-973
CloneExpress II One Step Cloning Kit	Vazyme	Cat#:C112
Cell Culture		
DMEM	Gibco	Cat#:C11995500BT

RPMI Medium Modified	HyClone	Cat#:SH30809.01
Cell Culture Flask/Dish	Nest biotechnology	/
Mouse: C57BL/6	Cyagen	
Oligonucleotides		
KLHL22 siRNA#1: 5′ - CAGGCTACGTGCACATTTA - 3′	Su Zhou Ji Ma (China)	
KLHL22 siRNA#2: 5′ - GCTCAACAACTTCGTATAC - 3′	Su Zhou Ji Ma (China)	
Primer: Human *PDCD1* forward: 5′- GACAGCGGCAC-CTACCTCTGTG -3′		
Primer: Human *PDCD1* reverse: 5′- GACCCAGACTAG-CAGCACCAGG -3′		
Primer: Human *KLHL22* forward: 5′- GAGAGTGGAAGC ACTTCACTG -3′		
Primer: Human *KLHL22* reverse: 5′- GCGTAGATGTAC-CTGCCTACA -3′		
Primer: Mouse *Pdcd1* forward: 5′- CGTCCCTCAG-TCAAGAGGAG -3′		
Primer: Mouse *Pdcd1* reverse: 5′- GTCCCTA-GAAGTGCCCAACA -3′		
Primer: Mouse *Klhl22* forward: 5′- TCTACCGGCTAG-CAGACCTC -3′		
Primer: Mouse *Klhl22* reverse: 5′- TGCAC-CTGCTCTAGGGAGTA -3′		
Recombinant DNA		
pDEST-C-SFB-PD-1/K210R/K233R mutant	This study	
pHBLV-C-Flag-PD-1	Hanbio Biotechnology	
pDEST-N-SFB-KLHL22/Δ6K mutant	This study	
pDEST-C-SFB-PD-L1	This study	
pDEST-N-SFB-KLHL9	This study	
pDEST-N-SFB-KLHL13	This study	
pDEST-N-SFB-KLHL19	This study	
pDEST-N-Myc-KLHL22/Δ6K mutant	This study	
pDEST-N-Myc-KLHL9	This study	
pDEST-N-Myc-KLHL13	This study	
Software and Algorithms		
Prism 8	GraphPad	https://www.graphpad.com/scientific-software/prism/
FlowJo V10	TreeStar	https://www.flowjo.com/solutions/flowjo/downloads
Servier Medical Art	Servier	https://smart.servier.com
Microsoft office Word/Excel/Powerpoint	Microsoft	https://office.live.com
Flourish.studio	Flourish	https://flourish.studio/

Other		
S protein Agarose	Merck Millipore	Cat#:69704
FLAG-M2 beads	Sigma-Aldrich	Cat#:M8823
Protein-A beads	GE life	Cat#:45002161
EasyTag Express Protein Labeling Mix, [^{35}S]-	PerkinElmer	Cat#:NEG772